

Kinetic Studies of Pristine and Nanonickel Catalyzed Ammonia Borane

Dileep Kumar^{1*}, H.A. Mangalvedekar¹, S.K. Mahajan², A.C. Gangal³

¹VJTI, Matunga (E), Mumbai, MS, India

²Directorate of Technical Education, 3 Mahapalika Marg, Mumbai, MS, India

³Gharda Institute of Technology, Chiplun, MS, India

Abstract

The high hydrogen content chemical hydride, Ammonia Borane (NH_3BH_3 , AB) is considered in its pure and catalyzed form for decomposition kinetics. The thermodynamics and slow kinetics are the major issues in addition to potential damage the material likely to cause to the fuel cell. The ability of AB for faster dehydrogenation at lower temperatures with Nickel in its nanoform is explored. The release kinetics, activation energy is computed using Kissinger and isoconversional models for AB and ABNi which is elaborated in the paper.

Keywords: Ammonia borane, nanonickel, dehydrogenation, kinetics, activation energy

*Author for Correspondence E-mail: dknayak@vpmthane.org

INTRODUCTION

Ammonia Borane (AB) is a nonvolatile material with good degree of stability in air and water under ambient conditions. It is a promising energy carrier for low power applications using PEMFC at lower temperatures. The neat AB exists in stable crystalline form with strong bond structure which is responsible for higher melting point of about 110 °C [1]. Merino *et al.* suggested that the strong electrostatic forces from dipole moments of the AB molecule are responsible for high melting point [2]. The optimum thermal decomposition reaction of ammonia borane, $\text{NH}_3\text{BH}_3 \rightarrow \text{BN} + 3\text{H}_2$ occurs by a three-step process with very high H_2 yields (19.6 wt%). This is far above the US DOE set goals. The reactions are not reversible and off board regeneration is needed for practical use of the material for mobile applications. Even if the first two steps prove feasible, H_2 capacities of over 12 wt% could be realized [3, 4]. The two steps, i.e., reaction of AB to form polyaminoborane $[(\text{NH}_2\text{BH}_2)_n]$, PAB; and PAB to form polyiminoborane $[(\text{NHBH})_n]$, PIB] amount to around 12 wt% hydrogen. The stringent requirements of hydrogen purity for fuel cell applications demand minimization of side reactions [4]. The possibility of gaseous boranes in the evolved H_2 is toxic and likely to poison the fuel cell catalyst. Above 500 °C,

AB can be completely decomposed to form boron nitride (BN). For spent fuel regeneration, BN is not preferred due to its high chemical and thermal stability [5]. AB is a widely studied material for its decomposition by thermolysis, hydrolysis and hydrothermolysis [6]. The thermolysis or direct heating is one of the methods of dehydrogenation. The main hurdle in hydrogen release is the slow kinetics, leading to long induction period [7]. Neat AB thermally decomposes initially at 70 °C, and reaches a maximum at 112 °C with the observed melting of AB to yield 1.1 ± 0.1 equiv. H_2 and byproduct PAB [8–10]. The PAB obtained can decompose over a broad temperature range between 110–200 °C to lose 1 equiv. H_2 and form PIB [8]. Solid state hydrogen is the contemplated safe method of storage. In this, hydriding materials are used for hydrogenation and dehydrogenation. Kinetics and operating temperatures play an important role as the performance of fuel cell depends on these parameters. AB is a disposable source with its dehydrogenation temperatures close to the operating temperature of PEMFCs. The hydrolysis or catalyzed thermolysis helps to further lower the dehydrogenation temperatures as well as to improve release kinetics offering adequate scope for experimental research. Most of the literature survey included the use of organic or

inorganic solvents for hydrolysis to observe performance improvements. The solid state thermolysis with nickel in its nanof orm as catalyst seems a good choice for thermolysis. The low cost, nonnoble metal nickel is chosen with the goal to improve hydrogen release kinetics.

EXPERIMENTAL

The experiments for dehydrogenation and kinetic analysis were conducted in two stages. First set of experiments were performed on pristine AB. AB purchased from Sigma Aldrich (97% pure) was used as received in very small samples. In the second stage of experimentation, the catalyzed AB samples were used for isothermal as well as nonisothermal studies. Nanonickel purchased from the Laboratory Chemical Co. was used in 10% quantity for mechanical mixing. The set of experiments performed on neat AB were repeated with ABNi samples for hydrogen release as well as kinetic studies. The experiments for isothermal decomposition were conducted in an indigenously developed Sievert's type apparatus. The samples were subjected to isothermal decomposition at temperatures 80 °C, 100 °C, 140 °C and 160 °C. The volume of the evolved gas w.r.t. time was recorded to compute wt% as well as α . The experimental data were used to plot PCI curves and α versus time for kinetic analysis. The pure AB samples were subjected to nonisothermal decomposition at heating rates of 3 °C/min, 4 °C/min and 5 °C/min from 20 °C to 250 °C. The DTA, TGA, differential thermogravimetric (DTG) curves and data were used for weight loss calculations, hydrogen release studies and kinetic analysis. The thermogravimetry and differential thermal analysis of neat and catalyzed AB samples was separately performed in Perkin Elmer TGDTA system.

THEORY

Chemical Reaction Kinetics

This is an extensive area dealing with the reaction rate w.r.t. time under isothermal or nonisothermal conditions. The objective of this analysis is to expect and explore faster kinetics. Kinetic behavior depends on operating conditions and types of controls. Solid state reaction takes place in one of the following ways:

- Diffusion of reactants to reactive surface.
- Adsorption at the reactive surface.
- A reaction on the atomic scale on the reaction surface.
- Nucleation of the product.
- Growth and diffusion of products away from the reactive surface.

The kinetic parameters include Activation Energy (E_a) and preexponential or frequency factor (A). E_a is defined as the energy that must be overcome in order for a chemical reaction to occur. It is also defined as the minimum energy required for starting the chemical reaction which is expressed in kJ/mol. For a chemical reaction to proceed with reasonable reaction rate there must be appreciable number of molecules with energy which is equal to or greater than the E_a . The preexponential factor which is also called as the frequency factor is often called the attempt frequency of reaction. ' A ' is the total number of collisions per second which may or may not lead to a reaction and ' k ' is the probability of collision occurring in a reaction. It may be noted that at lower reaction fraction, the activation energy will be higher and as the reaction extent increases, the activation energy requirement decreases.

Thermal Analysis (TA)

The extraction of relevant information from isothermal and nonisothermal data using TA techniques and the modeling of the kinetic process is the important function of analysis. The aim of kinetic analysis of thermal decomposition data is to choose the best model to describe the analyzed process and importantly obtain reliable parameters E_a and A which are correlated mutually. Any change in E_a has to be compensated by A {change in $\ln A$ } as represented in $\ln A = a + b E_a$ where a and b are constants [11].

Types of Models

The kinetics of solid state reactions is studied with one of the following models [12]:

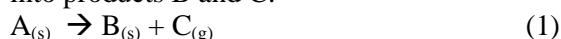
Diffusion Model: This model is applicable when reaction takes place between two solids with reactants in separate crystal lattices. Diffusion plays an important role in controlling the rate of reaction which is controlled by the movement of reactants to

products from the reaction interface as the product layer increases.

Geometrical Concentration Model: This model assumes that the reaction occurs rapidly on the surface of the crystal. The rate of reaction is controlled by the reaction interface progress toward the centre of the crystal. The model changes with the shape of the crystal.

Reaction Order-Based Model: This is one of the applicable models of solid state reactions. Using the rate of reaction, rate constant and order of the reaction, it is possible to obtain kinetic parameters based on the order of reaction.

Nucleation Model [13]: Nucleation can be defined as the phenomenon of formation of a new product from the reactant phase. The solid state reactions such as decomposition/dehydrogenation etc. follow the nucleation/Kissinger's model. In this model, the solid reactant A decomposes completely into products B and C.



The solid state reactions are studied with variety of models and for elaboration it was necessary to detail few of the models. The models are listed as a part of theoretical study. AB dehydrogenation follows the model as the reaction steps are assumed to follow in Eq. 1. Depending on the type of chemical reaction, it

is essential to identify one of the suitable models for kinetic analysis. Some of the models recommended for analysis based on the type of solid state reaction are listed in Table 1.

The experimentally obtained reaction fraction α as a function of time is the basis of kinetic studies.

The type of reaction encountered while using AB is related to nucleation/Kissinger's model. The isoconvensional or model-free method recommended by Gangal and Sharma [11] seems equally appropriate for the nonisothermal analysis. The analysis has indicated substantial reduction in E_a with catalyzed samples.

Computation of E_a using Kissinger's Analysis

E_a can be found based on multiple scan methods with several measurements of different heating rates. The values of E_a of AB and ABNi from some of the earlier literature are listed below:

Literature survey for E_a values from various models is listed in Table 2. It may be noted from Table 2, that the pristine AB E_a is found to be in the range of 160–184 kJ/mol with different models. The Ni catalyzed AB dehydrogenation process indicated the reduction in E_a to 123.5 kJ/mol.

Table 1: Kinetic Models for Solid State Reactions [14].

Model	Order/ Dimension	Differential form $f(\alpha)$	Integral form $g(\alpha)$
Diffusion model	D1	$1/2\alpha$	α^2
	D2	$[-\ln(1-\alpha)]-1$	$[(1-\alpha)\ln(1-\alpha)]+\alpha$
	D3	$3(1-\alpha)^{2/3}+[1-(1-\alpha)^{1/3}]$	$[1-(1-\alpha)^{1/3}]^2$
Diffusion G-B	D4	$[3/2(1-\alpha)^{-1/3}-1]$	$1-(2\alpha/3) - (1-\alpha)^{2/3}$
Zero order	F0	1	α
First order	F1	$1-\alpha$	$-\ln(1-\alpha)$
Second order	F2	$(1-\alpha)^2$	$(1-\alpha)^{-1} - 1$
Third order	F3	$(1-\alpha)^3$	$0.5(1-\alpha)^{-2} - 1$
Prout Tomkins Power law	P2	$(2\alpha)^{1/2}$	$(\alpha)^{1/2}$
	P3	$(3\alpha)^{2/3}$	$(\alpha)^{2/3}$
	P4	$(4\alpha)^{3/4}$	$(\alpha)^{3/4}$
Avrami-Erofeyev	A2	$2(1-\alpha)[- \ln(1-\alpha)]^{1/2}$	$[- \ln(1-\alpha)]^{1/2}$
	A3	$3(1-\alpha)[- \ln(1-\alpha)]^{2/3}$	$[- \ln(1-\alpha)]^{1/3}$
	A4	$4(1-\alpha)[- \ln(1-\alpha)]^{3/4}$	$[- \ln(1-\alpha)]^{1/4}$

Table 2: Literature Survey for E_a Values from Various Models.

Material	E_a (kJ/mol)	Model
Ammonia Borane	181.7	Kissinger's method [15]
	184	Isothermal DSC [16]
	160	Kissinger's nonisothermal DSC [17]
	183	Arrhenius [18]
AB + 2% Ni	123.5	Kissinger's plot [19]

The Kissinger's method/analysis is based on maximum rate on a TA curve. Arrhenius equation is a simple and reasonably accurate expression for understanding of the temperature dependence of reaction rates. This gives the dependence of the rate constant k of a chemical reaction on temperature T (Kelvin), A is the preexponential factor or the frequency factor, E_a is the activation energy and R is the universal gas constant. The rate constant is expressed as,

$$k = Ae^{\frac{-E_a}{RT}} \quad (2)$$

Function $f(\alpha)$ represents the mathematical expression of kinetic model.

Differential form of rate of reaction can be expressed as,

$$\frac{d\alpha}{dt} = Ae^{\frac{-E_a}{RT}} f(\alpha) \quad (3)$$

The maximum rate of reaction can be obtained by double differentiation and equating to zero

$$\frac{d^2\alpha}{dt^2} = \left(\frac{E_a e}{RT_m^2} + Af'(\alpha_m) e^{\frac{-E_a}{RT_m}} \right) \left(\frac{d\alpha}{dt} \right)_m = 0 \quad (4)$$

Where,

β = Constant heating rate

T_m = Temperature at which maximum reaction rate is observed

α_m = Maximum reaction fraction

Taking natural logarithm on either sides,

$$\ln\left(\frac{\beta}{T_m^2}\right) = \ln\left(\frac{-AR}{E_a} f'(\alpha_m)\right) - \frac{E_a}{RT_m} \quad (5)$$

For a first order reaction

$$f'(\alpha) = -1$$

we get,

$$\ln\left(\frac{\beta}{T_m^2}\right) = \ln\left(\frac{AR}{E_a}\right) - \frac{E_a}{RT_m} \quad (6)$$

The plot of $\ln(\beta/T_m^2)$ against $(1/T_m)$ is used to estimate E_a and the preexponential factor A . We can find the values of T_m from DTG curves of AB and ABNi for various heating rates β .

Isoconversional or Model-free Method

This method uses isothermal data for estimation of A and E_a . The integral form of equation is given by,

$$g(\alpha) = kt \quad (7)$$

Substituting for k from Eq. (2) we get,

$$g(\alpha) = Ae^{\frac{-E_a}{RT}} \cdot t \quad (8)$$

Taking natural logarithm on both the sides

$$-\ln(t) = \ln(A) - \ln(g(\alpha)) - \frac{E_a}{RT} \quad (9)$$

The value of $\ln(g(\alpha))$ is negligible and hence Eq. (9) is rewritten as

$$-\ln(t) = \ln(A) - \frac{E_a}{RT} \quad (10)$$

We can obtain E_a and A from plot $-\ln(t)$ versus $1/T$ for specific value of α .

As the value of α increases, E_a and A will decrease due to isothermal nature of the reaction.

RESULTS AND DISCUSSION

The kinetic analysis is an important part of our investigation to justify our claim of improvement of dehydrogenation performance of AB with nonnoble metal nickel catalyst in its nano form. We have seen significant reduction in induction period and considerable increase of hydrogen gas with the use of catalyst in the isothermal studies of AB and ABNi. By treating the data obtained in isothermal & nonisothermal experimentation, we have made an attempt to obtain kinetic parameters.

Nonisothermal Analysis

For the study of reaction kinetics, we have used Arrhenius equation and Kissinger's method. The DTG data obtained from the TGDTA experiment is used for plotting the DTG curve. The heating program was conducted from 20 °C to 250 °C with heating rates of 3 °C/min, 4 °C/min and 5 °C/min. The heating rates were chosen to study the TGA, DTA and DTG characteristics with lower rates

for both AB and ABNi samples. The curves are distinctly visible for each heating rate with the curve shifting towards right with increase in heating rate. Owing to clarity of data, computation of E_a is performed using Arrhenius plot. The set of DTG curves obtained for AB and ABNi samples is shown in Figures 1 and 2.

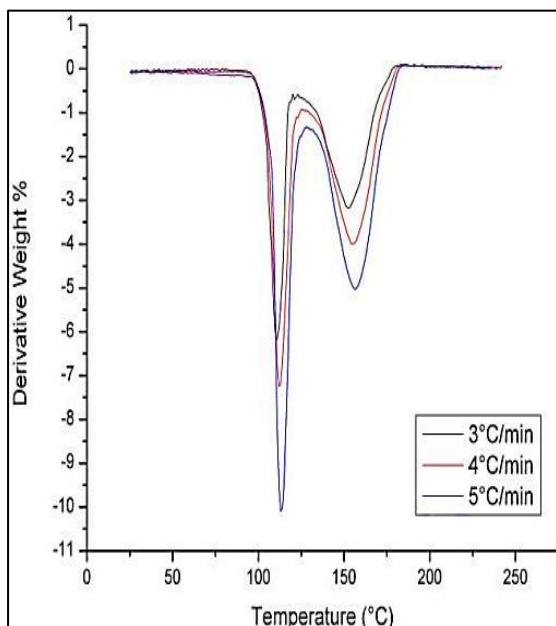


Fig. 1: DTG Curve of AB.

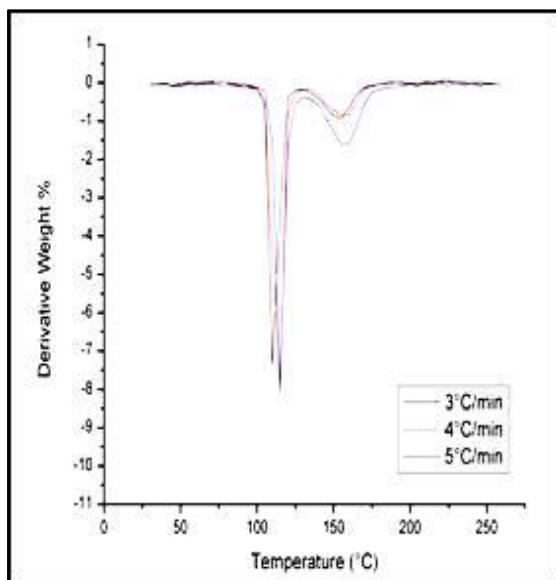


Fig. 2: DTG Curve of ABNi.

Table 3 indicates the values of T_m for different heating rates from the above DTG curves. Arrhenius plot of $-\ln(\beta/T_m^2)$ versus $1/T_m$ is used to compute E_a and frequency factor.

Table 3: DTG Maximum Reaction Rate Temperatures in °C for AB and ABNi.

Heating rate (β)	AB T_m	ABNi T_m
3	110.5	112.06
4	112.4	113.55
5	113.3	115.82

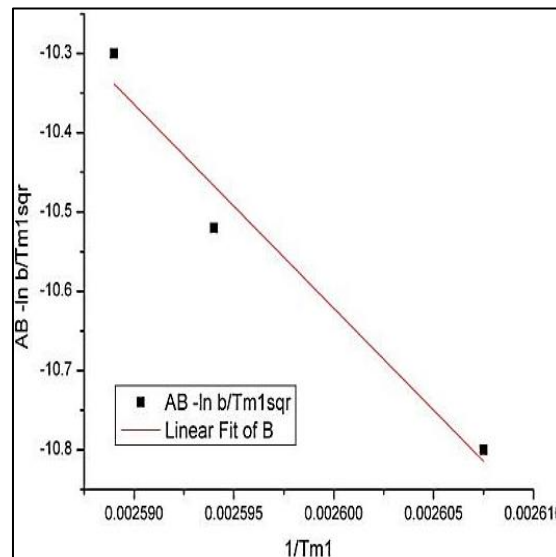


Fig. 3: Arrhenius Plot of AB T_m1 .

The value of E_a is found to be 213 ± 41 kJ from Figure 3 along with frequency factor 6.78×10^{28} .

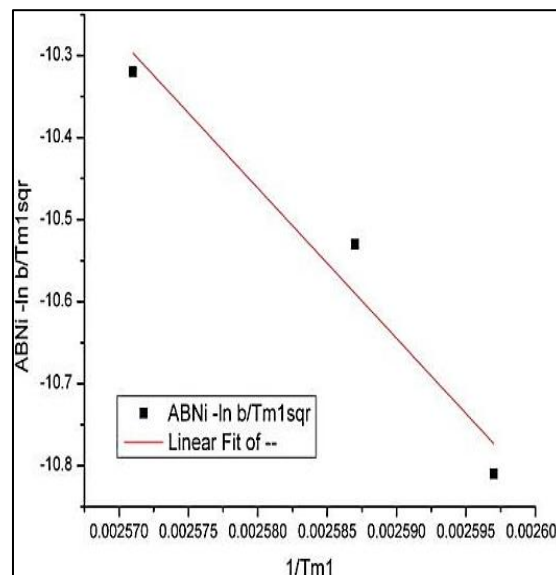


Fig. 4: Arrhenius Plot of ABNi T_m1 .

The ABNi sample E_a is computed to be 152 ± 33.2 kJ with frequency factor 1.73×10^{20} (Figure 4).

Isoconversional Method and Analysis

This is an alternate technique to compute kinetic parameters. It is also known as model-free fitting. In this technique, the reaction fraction α is computed for each reading in isothermal dehydrogenation step. Using this data, α versus t plot is obtained as shown in Figures 5 and 6.

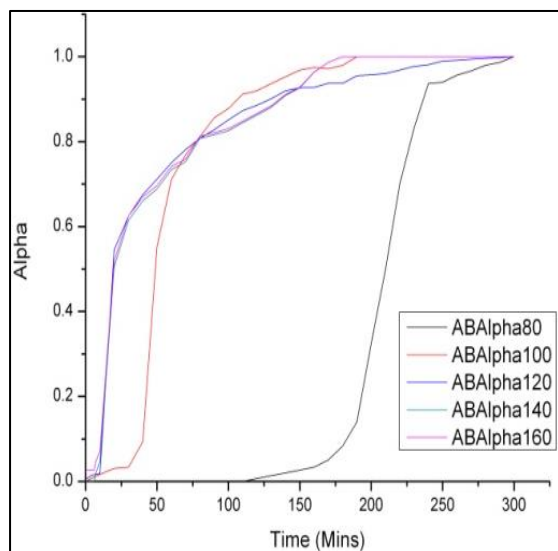


Fig. 5: Isoconversional Alpha (α) vs. Time Plot for AB.

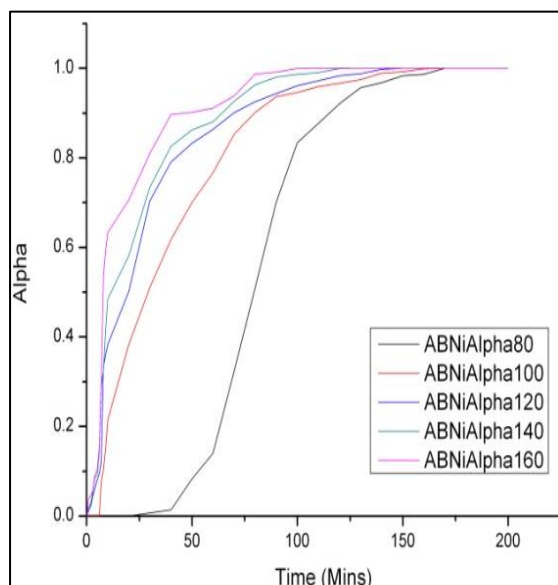


Fig. 6: Isoconversional Alpha (α) vs. Time Plot for ABNi.

The above plot is a result of analysis obtained from the previous values. For different values of α from 0.1 we obtained corresponding value of t to obtain $-\ln(t)$ versus $1/T$. The E_a values from this method are listed in Table 4.

Table 4: α vs. E_a of AB and ABNi.

α	AB		ABNi	
	(A/sec)	E_a (kJ/mol)	A/sec	E_a (kJ/mol)
0.1	28.2×10^8	45.91 ± 9.33	1.6×10^8	34.23 ± 12.17
0.2	11.5×10^8	43.33 ± 9.25	1.3×10^8	34.10 ± 11.88
0.5	2.3×10^8	39.20 ± 10.40	4.8×10^6	33.09 ± 4.05
0.8	3.08×10^3	16.18 ± 6.80	1.7×10^4	19.18 ± 1.20

For this method, we have chosen the values of $\alpha=0.1, 0.2, 0.5$ & 0.8 for the calculation of kinetic parameters. The values of E_a and frequency factor are listed in Table 4.

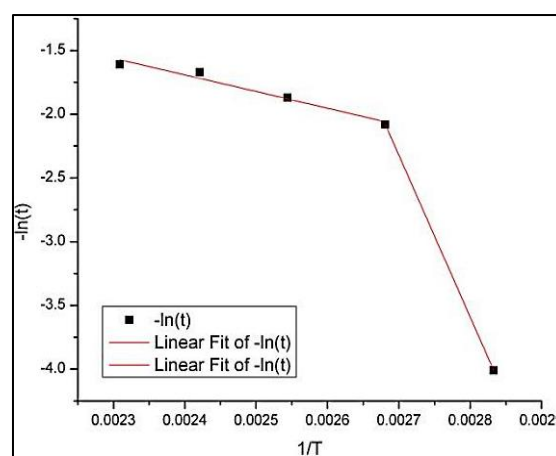


Fig. 7: ABNi Arrhenius Plot of $-\ln(t)$ vs. $1/T$ with Alpha = 0.1.

The above plot (Figure 7) indicates the isoconversional or model-free fitting analysis. The first mole release occurs between 80 °C to 110 °C and the E_a was found to be 107.81 kJ with frequency factor of 1.0×10^{18} which is much lower than the neat AB value. The second reaction step is assumed to have occurred between 110 °C and 160 °C. The E_a computed from the plot is 34.48 ± 1.40 kJ with frequency factor of 17.692×10^3 . It could be seen that both the steps of hydrogen release occurred at much lower energy levels indicating the effect of catalysis.

CONCLUSION

The solid state reaction kinetic analysis is performed using Kissinger's method and isoconversional method. The chosen catalyst nickel in its nano form has indicated the reduction in induction time in isothermal dehydrogenation as well as increase in hydrogen release at considered temperatures when compared with neat AB. The Kissinger's

analysis indicated the E_a of 215 kJ for neat AB and 152 kJ for ABNi. We can infer that there is decrease in E_a for the catalyzed sample. Even the model-free fitting method is indicating substantial reduction in E_a and A . It can be inferred that nanonickel as catalyst modified the transition state to lower the E_a .

REFERENCES

1. Weaver JR, Shore SG, Parry RW. The dipole moment of ammonia-borane. *J Chem Phys.* 1958; 29(1): 1–2p.
2. Merino G, Bukhmov VI, Vela A. Do cooperative proton-hydride interactions explain the gas-solid structural difference of BH_3NH_3 ? *J Phys Chem.* 2002; 106: 8491–4p.
3. Riis T, Sandrock G. Hydrogen storage gaps and priorities. *HIA HCG Storage paper.* 2005; 11: 1–11p.
4. Autrey T, Gutowska A, Li L, *et al.* Chemical hydrogen storage in nano-structured materials, control of hydrogen release and reactivity from ammonia borane complexes. *J Am Chem Soc Div Fuel Chem.* 2004; 49(1): 150–51p.
5. Diwan M, Hwang HT, Al-Kukhun A, *et al.* Hydrogen generation from noncatalytic hydrothermolysis of ammonia borane for vehicle applications. *AIChE J.* 2011; 57: 259–64p.
6. Gangal AC, Kale P, Edla R, *et al.* Study of kinetics and thermal decomposition of ammonia borane in presence of silicon nanoparticles. *Int J Hydrog Energy.* 2012; 37(8): 6741–8p.
7. Dileep K, Mahajan SK, Mangalvedekar HA. Hydrogen storage in amine borane complexes. *Proceedings of the 3rd International Conference on Fuel Cell and Hydrogen Technology ICFCHT.* 2011 Nov 22–23; Kuala Lumpur, Malaysia. 1–5p.
8. Peng B, Chen J. Ammonia borane as an efficient and lightweight hydrogen storage medium. *Energy Environ Sci.* 2008; 1: 479–83p.
9. Stowe AC, Shaw WJ, Linehan JC, *et al.* In situ solid state ^{11}B MAS-NMR studies of the thermal decomposition of ammonia borane: mechanistic studies of the hydrogen release pathways from a solid state hydrogen storage material. *Phys Chem Chem Phys.* 2007; 9: 1831–6p.
10. Sit V, Geanangel RA, Wendlandt WW. The thermal dissociation of NH_3BH_3 . *Thermochim Acta.* 1987; 113: 379–82p.
11. Gangal AC, Sharma P. Kinetic Analysis and Modeling of Thermal Decomposition of Ammonia Borane. *Int J Chem Kinetics.* 2013; 45(7): 452–61p.
12. Garner WE. *Chemistry of Solid State.* New York: Academic Press; 1955.
13. Khawam A, Flanagan DR. Solid-State Kinetic Models: Basics and Mathematical Fundamentals. *J Phys Chem B.* 2006; 110: 17315–28p.
14. Brown ME, Galwey AK. The Distinguishability of Selected Kinetic Models for Isothermal Solid-State Reaction. *Thermochim Acta.* 1979; 29: 129–46p.
15. Heldebrant DJ, Karkamkar A, Hess NJ, *et al.* The effect of chemical additives on induction phase in solid-state thermal decomposition of ammonia borane. *Chem Mater.* 2008; 20: 5332–6p.
16. Gutowska A, Li L, Shin Y, *et al.* Nanoscaffold mediates hydrogen release and reactivity of Ammonia Borane. *Angew.Chem Int Ed.* 2005; 44: 3578–82p.
17. Sepheri S, Garcia BB, Cao G. Tuning dehydrogenation temperature of Carbon-Ammonia Borane nanocomposites. *J Mater Chem.* 2008; 18: 4034–7p.
18. Kang X, Fang Z, Kong L, *et al.* Ammonia Borane destabilised by Lithium Hydride: An advanced on-board hydrogen storage material. *Adv Mater.* 2008; 20: 2756–9p.
19. He T, Xiong Z, Wu G, *et al.* Nanosized Co- and Ni-catalyzed ammonia borane for hydrogen storage. *Chem Mater.* 2009; 21: 2315–18p.

Cite this Article

Kumar D, Mangalvedekar HA, Mahajan SK, Gangal AC. Kinetic Studies of Pristine and Nanonickel catalyzed Ammonia Borane. *Journal of Alternate Energy Sources & Technologies.* 2015; 6(1): 7–13p.